



Influence of low and high IFT fluid systems on scaling parameters of laboratory modelling of CO₂ injection into saline aquifers

The 6th Trondheim Conference on CO₂ Capture, Transport, and Storage
14-16 June 2011, Trondheim, Norway

Szczepan Polak^{a,b,*}, Torleif Holt^b, and Ole Torsæter^a

^aDepartment of Petroleum Engineering and Applied Geophysics,
Norwegian University of Science and Technology (NTNU), NO-7491 Trondheim, Norway

^bSeismic and Reservoir Technology Department, SINTEF Petroleum Research,
P.O. Box 4763 Sluppen, NO-7465 Trondheim, Norway

*corresponding author; e-mail address: szczepan.polak@sintef.no

Content

1. Objectives
2. Method
3. Experiments
4. Results
5. Summary

Content

1. Objectives
2. Method
3. Experiments
4. Results
5. Summary

Objectives

- Understand the flow processes that take place within the reservoir during CO₂ injection.
- Experimentally investigate the scaling laws which describe CO₂ injection into saline aquifers.
- Demonstrate the influence of gravitational, viscous and capillary effects on the vertical flow of CO₂.

Content

1. Objectives
2. Method
3. Experiments
4. Results
5. Summary

Method

- Synthetic porous medium - two vertical glass plates with space between them packed with glass beads (Figure 1 and Table 1).

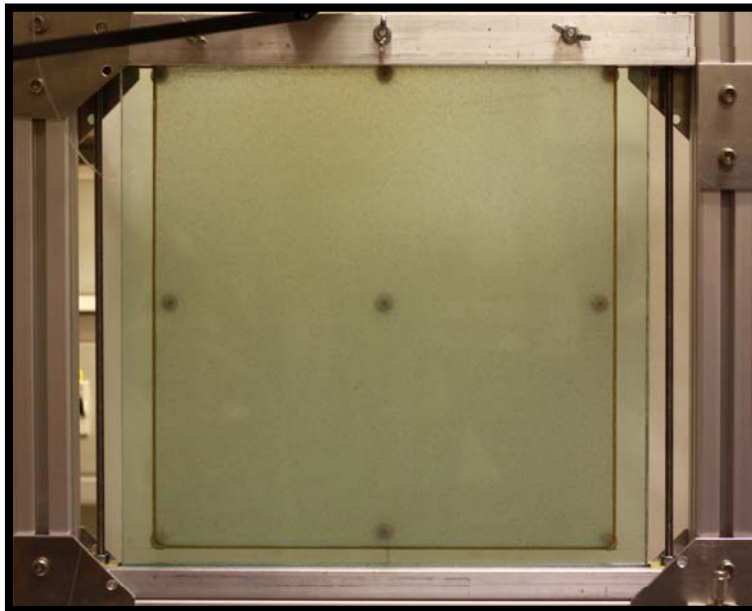


Figure 1. Model filled with glass beads.

Table 1. Physical properties of the model.

Height [cm]	30
Width [cm]	30
Distance from inlet to top of the model [cm]	28
Thickness [cm]	0.26
Porosity	0.39

Method

- The red-dyed CO₂-like phase injected at a constant rate into the model saturated with the brine-like phase (ambient conditions).
- Fluid systems, permeability, and injection rate were varied (Table 2).

Table 2. Sets of experimental parameters.

Case	Case description	Glass bead diameter, d [mm]	Porosity, ϕ	Permeability, k [D]	Flow rate, q [cm ³ /min]
1A	high IFT, low k, low q	0.2	0.39	40.2	0.10
1B	high IFT, low k, mid q	0.2	0.39	40.2	0.25
1C	high IFT, low k, high q	too high injection pressure			
2A	high IFT, high k, low q	0.4	0.39	161.0	0.10
2B	high IFT, high k, mid q	0.4	0.39	161.0	0.25
2C	high IFT, high k, high q	0.4	0.39	161.0	0.50
3A	low IFT, high k, low q	0.3-0.4	0.39	123.3	0.10
3B	low IFT, high k, mid q	0.3-0.4	0.39	123.3	0.25
3C	low IFT, high k, high q	0.3-0.4	0.39	123.3	0.50

Method

- Two sets of fluids used:
 1. High IFT – water, n-heptane, and glycerol,
 2. Low IFT – water, CaCl₂, iso-propanol, and iso-octane.
- Both mixtures separate into two phases at ambient conditions (Table 3).

Table 3. Properties of fluids used in experiments.

System	Fluid	Density [kg/m ³]	Density difference [kg/m ³]	Viscosity [mPa·s]	IFT [mN/m]
High IFT	glycerol-rich phase (BRINE)	1160.4	475.9	12.557	34.0
	n-heptane-rich phase (CO ₂)	684.5		0.408	
Low IFT	water-rich phase (BRINE)	903.1	205.6	3.556	1.0
	iso-octane-rich phase (CO ₂)	697.5		0.556	

Content

1. Objectives
2. Method
3. Experiments
4. Results
5. Summary

Experiments

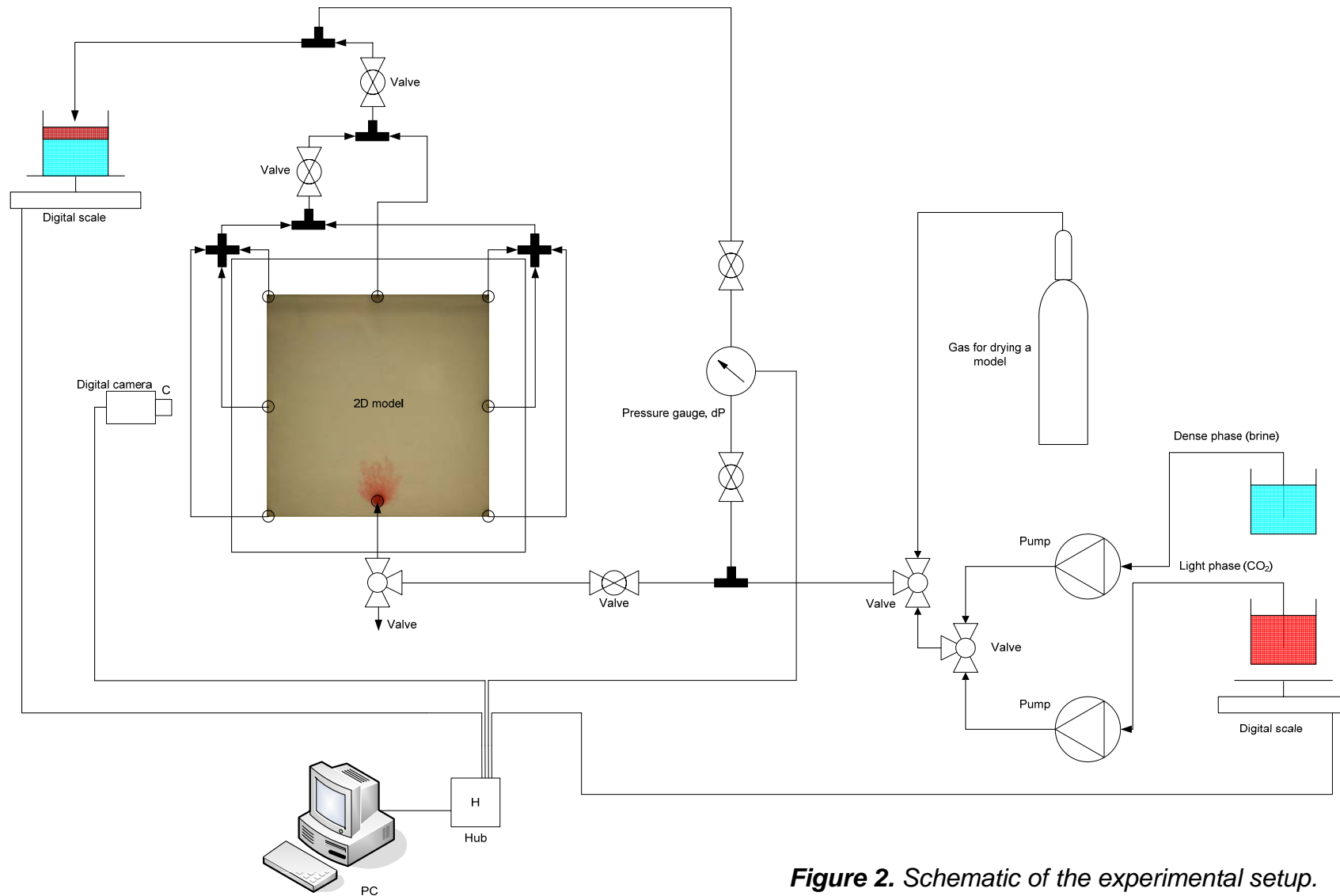


Figure 2. Schematic of the experimental setup.

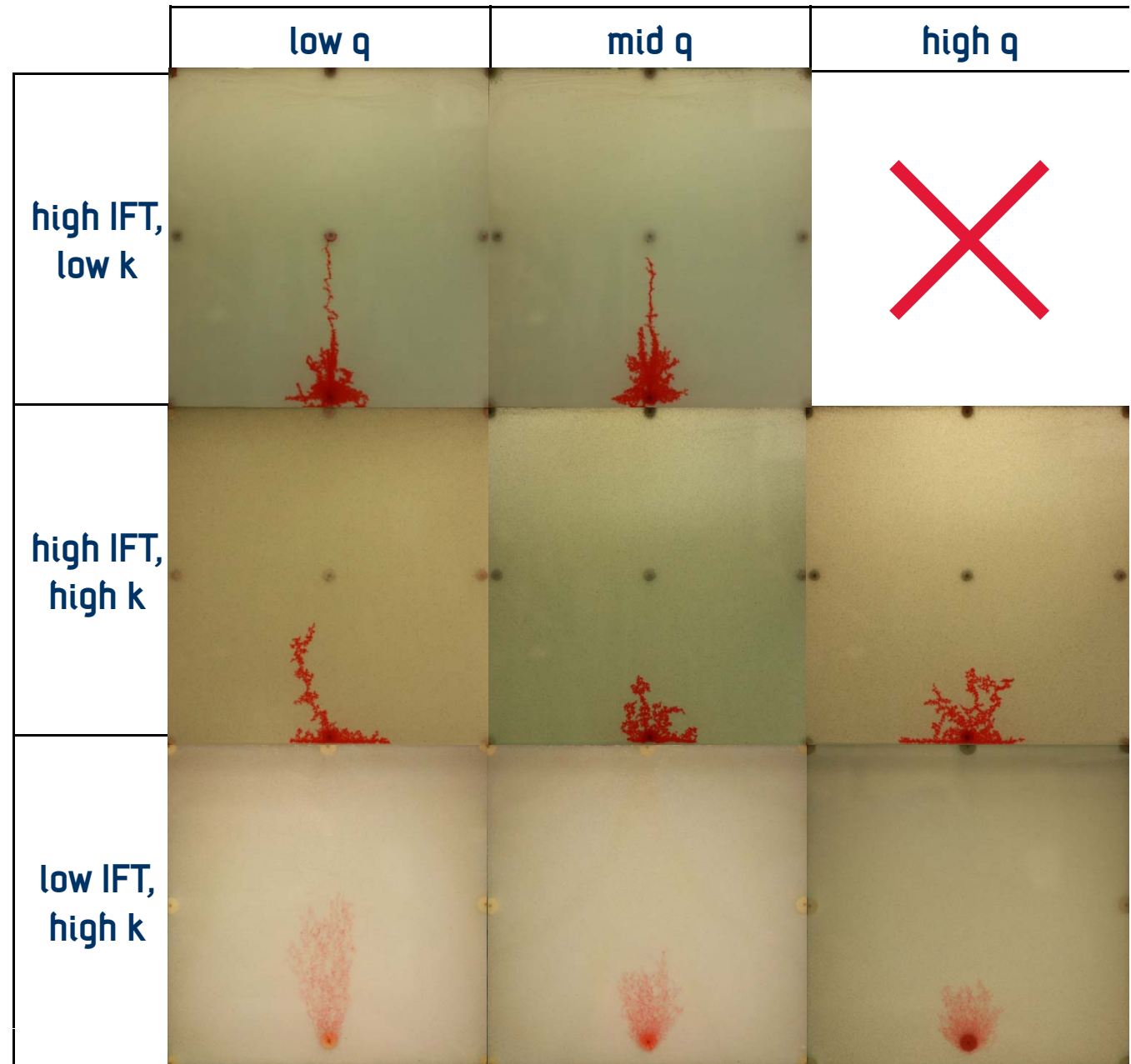
Experiments

Pictures taken at:

0.01 PV
injected

- The lower the injection rate – the narrower the plume.
- The higher the injection rate – the more of viscous fingering.

Figure 3a. Examples of saturation maps at different stages of displacements. Figures are representative for experiments within each case.



Experiments

Pictures taken at:

breakthrough

- Injected fluid reaches the top and starts leaving the model.

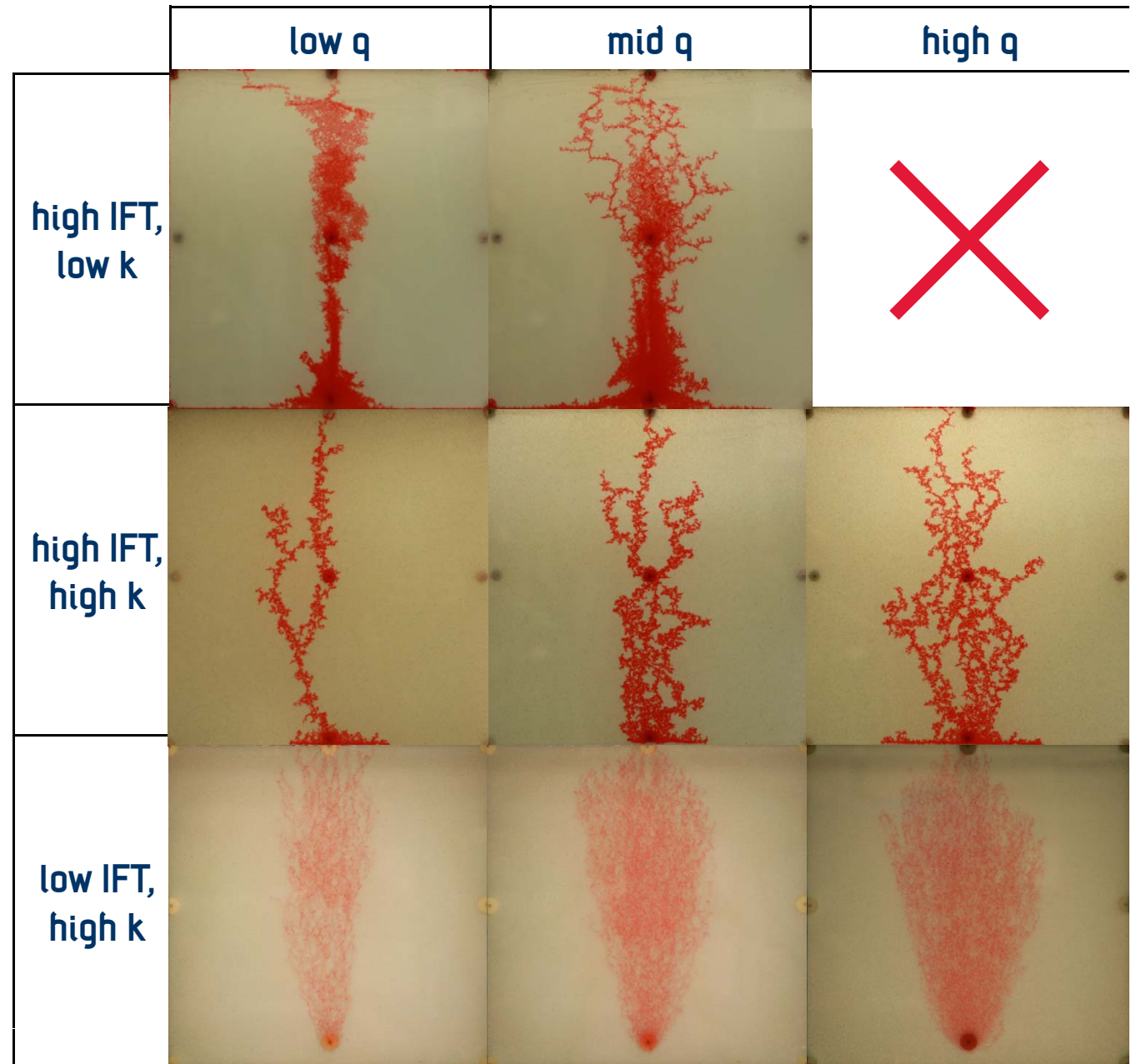


Figure 3b. Examples of saturation maps at different stages of displacements. Figures are representative for experiments within each case.

Experiments

Pictures taken at:

0.10 PV
injected

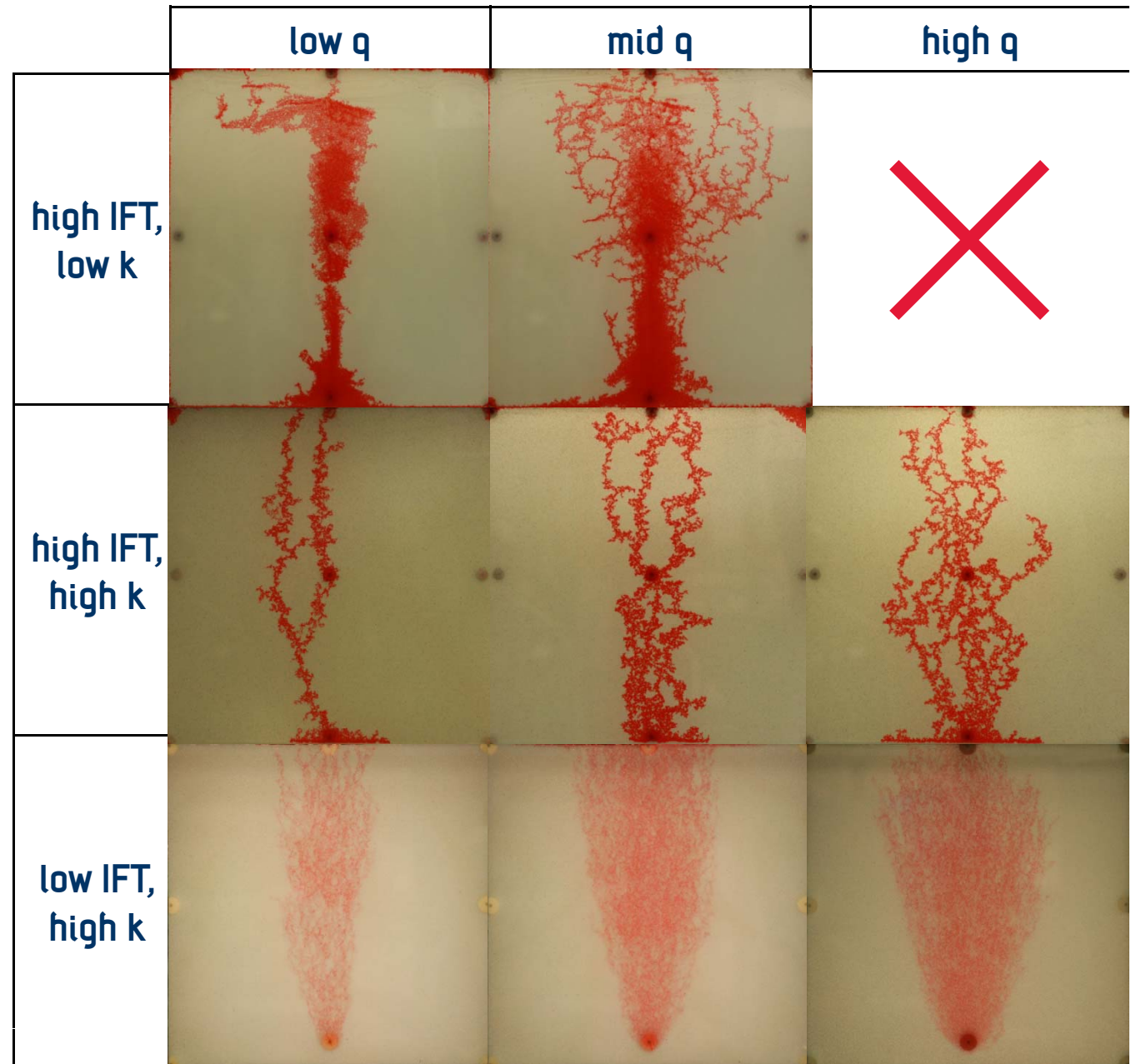


Figure 3c. Examples of saturation maps at different stages of displacements. Figures are representative for experiments within each case.

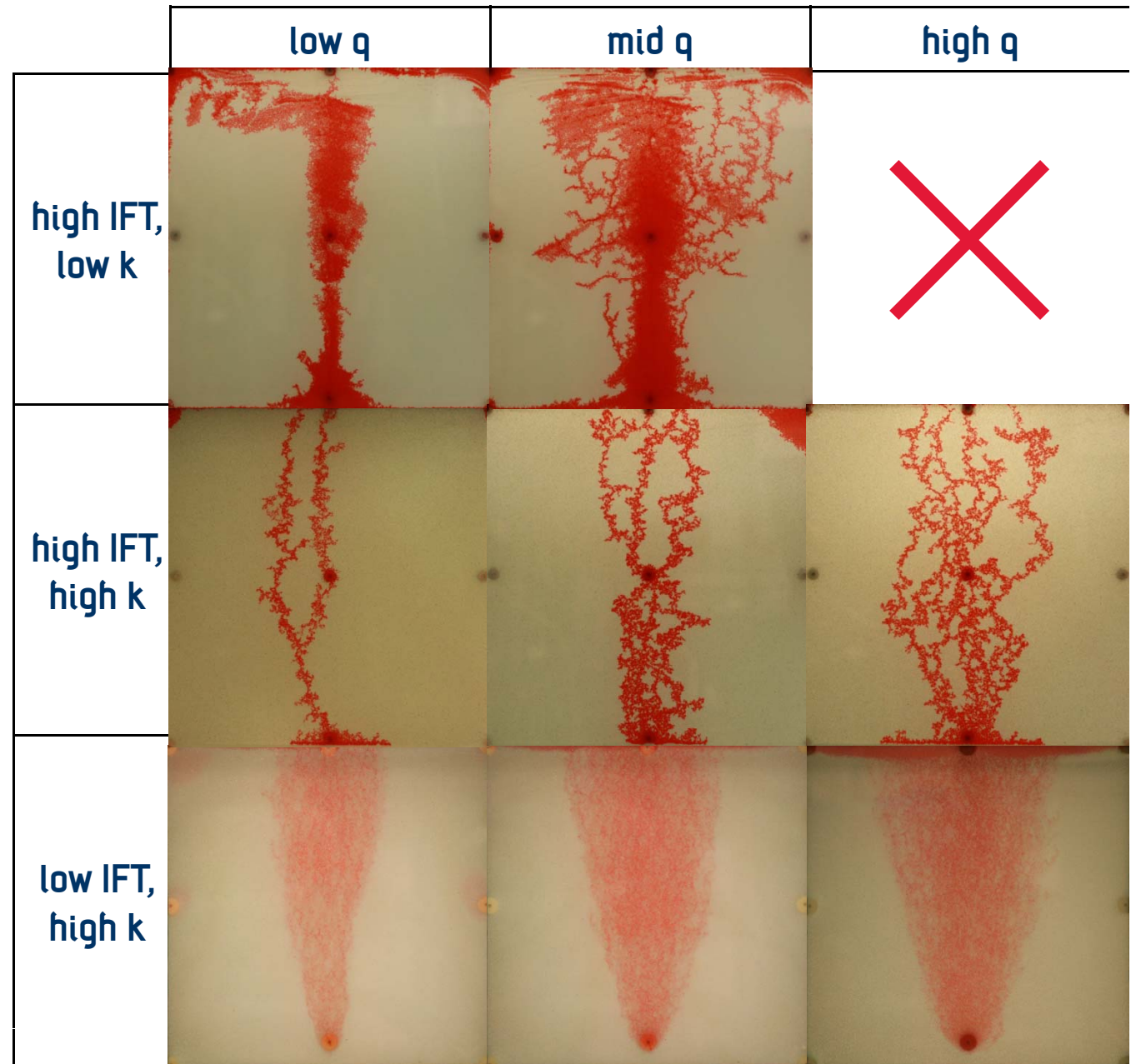
Experiments

Pictures taken at:

**0.25 PV
injected**

- Impact of viscous forces was stronger when injection rate was higher resulting in a larger plume.

Figure 3d. Examples of saturation maps at different stages of displacements. Figures are representative for experiments within each case.



Content

1. Objectives
2. Method
3. Experiments
4. Results
5. Summary

Results

- Increased injection rate results in higher recovery (Figure 4, 'C' cases).
- Low k cases have higher sweep efficiency comparing to high k (Figure 4, '1' vs. '2' cases).
- Low IFT cases have higher sweep efficiency comparing to high IFT cases (Figure 4, '3' vs. '2' cases).
- High sweep efficiency however, corresponds to the increased injection pressure.

Case	Case description
1A	high IFT, low k , low q
1B	high IFT, low k , mid q
2A	high IFT, high k , low q
2B	high IFT, high k , mid q
2C	high IFT, high k , high q
3A	low IFT, high k , low q
3B	low IFT, high k , mid q
3C	low IFT, high k , high q

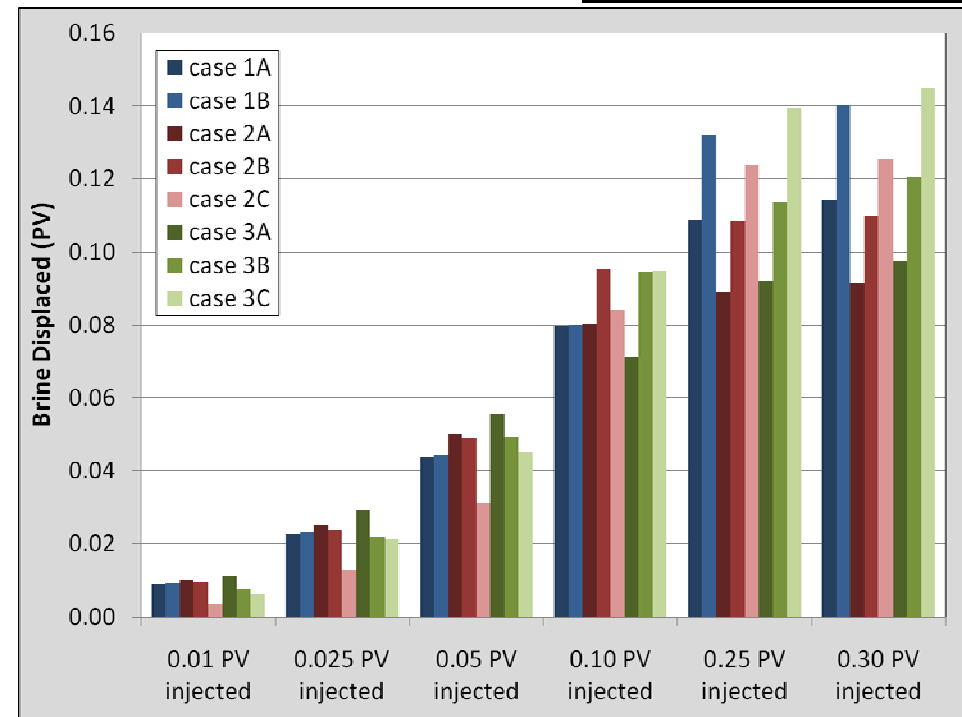


Figure 4. Brine displacement (averaged values).

Results

- Experiments are described by dimensionless capillary (N_c) and capillary-to-gravity-ratio (CGR) numbers which incorporate fluid and porous media (rock) properties (Table 4).

$$N_c = \frac{\mu_i \cdot u}{\gamma}$$

Table 4. Dimensionless numbers calculated for the experiments.

Case	Case description	CGR	N_c ($\cdot 10^{-3}$)	$N_c \cdot \text{CGR}$ ($\cdot 10^{-3}$)
1A	high IFT, low k, low q	4.8440	0.0642	0.3110
1B	high IFT, low k, mid q	4.8440	0.1605	0.7776
1C	high IFT, low k, high q	too high injection pressure		
2A	high IFT, high k, low q	2.4220	0.0642	0.1555
2B	high IFT, high k, mid q	2.4220	0.1605	0.3888
2C	high IFT, high k, high q	2.4220	0.3210	0.7776
3A	low IFT, high k, low q	0.1992	1.5060	0.3000
3B	low IFT, high k, mid q	0.1992	3.7650	0.7500
3C	low IFT, high k, high q	0.1992	7.5301	1.5001

$$\text{CGR} = \frac{2\gamma}{\Delta\rho \cdot g \cdot h \cdot \sqrt{\frac{k}{\phi}}}$$

- μ_i - viscosity of injected fluid, Pa·s
- u - injection velocity, m/s
- γ - interfacial tension, N/m
- $\Delta\rho$ - density difference of fluids, kg/m³
- g - acceleration of gravity, m/s²
- h - distance between model's inlet and outlet, m
- k - permeability, m²
- ϕ - porosity

Results

- Generally, brine displacement decreases with rising gravity forces (Figure 5).
- Lower injection rate means stronger gravity forces (Figure 5, 'A' cases).
- Larger density difference between fluids increases influence of gravity forces (Figure 5, '2' and '3' cases).
- Later breakthrough = more brine displaced = larger volume of the reservoir penetrated by injected fluid – favourable for CO₂ storage – more CO₂ can be dissolved during injection.

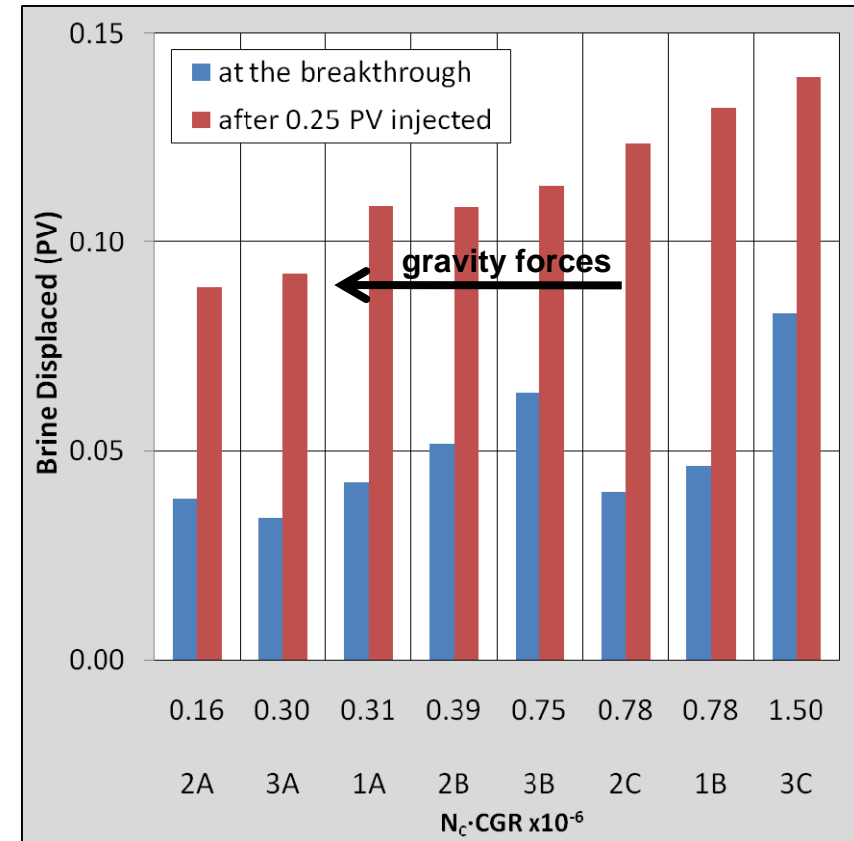


Figure 5. Dimensionless numbers vs. recovery.

Results

- CGR and N_c were calculated for the experiments and field cases.
- Laboratory experiments are dominated by viscous and especially capillary forces (particularly in high IFT system).
- Experimental CGR and $CGR \cdot N_c$ agree reasonably well with calculations for generic sedimentary basins (from Nordbotten, 2005) and some of the existing storage sites (Figure 6).
- Low IFT system scales closer to the existing storage sites than high IFT system.

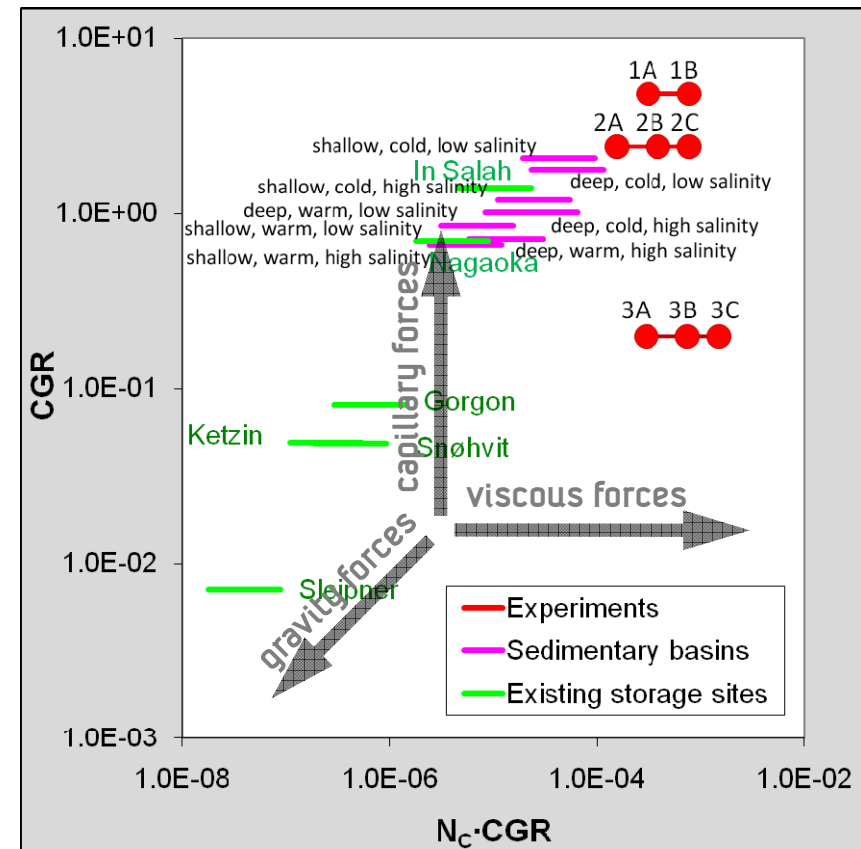


Figure 6. Representation of the experimental and field data by N_c and CGR. Forces that govern fluid flow in the reservoir.

Content

1. Objectives
2. Method
3. Experiments
4. Results
5. Summary

Summary

- Experiments show the plume development and the flow patterns of injected fluid from the start of injection until it reaches the top of the model reservoir.
- Flow paths are shorter in high-permeability cases than in low-permeability cases.
- Experiments are dominated by viscous and capillary forces.
- Viscous forces increased at higher injection rate:
 - more fingering,
 - increased total displacement.
- Gravity effects strongest at low injection rate and high permeability:
 - flow more in the vertical direction,
 - brine displacement decreases as the gravity forces are rising.

Summary

- Dimensionless numbers link the laboratory experiments with the field scale observations.
- Comparison of the scaling calculations for the experiments with calculations for the storage sites shows reasonably well match.
- Calculations for the low IFT fluid system scale closer to the field parameters, and high IFT system match better with generic reservoirs.

Future work

- Experiments
 - Optimize experimental setup, including porous medium and fluids, in order to obtain better match with field parameters.
- Numerical simulations
 - Modelling of the experiments,
 - Upscaling to the field-scale.

Acknowledgements

- This work is a part of the PhD project 'Storage of CO₂ in aquifers. Description of the fluid flow in the CO₂-water system.'
PhD candidate: Szczepan Polak (SINTEF Petroleum Research, NTNU)
project supervisor: professor Ole Torsæter (NTNU);
project co-supervisor: Torleif Holt, senior research scientist (SINTEF Petroleum Research)
- The author gratefully acknowledges SINTEF Petroleum Research and The School of Petroleum Engineering (UNSW) for making their facilities available to perform this research. The author also acknowledges the funding provided by the Australian Government through the CRC Program to support CO2CRC research.
- The PhD project is a part of the BIGCO2 project, performed under the strategic Norwegian research program CLIMIT. The author acknowledges the partners: Statoil, GE Global Research, Statkraft, Aker Clean Carbon, Shell, TOTAL, ConocoPhillips, ALSTOM, the Research Council of Norway (178004/I30 and 176059/I30) and Gassnova (182070) for their support.



CRC for Greenhouse Gas Technologies

